AFRL-AFOSR-UK-TR-2022-0031

Simultaneous and Synchronous Full Field Deformation and Temperature Measurements in High Rate Events

Hokka, Mikko
Tampereen korkeakoulusäätiö sr
Kalevantie 4
TAMPERE, Pirkanmaa, , 33100
FI

03/10/2022
Final Technical Report

Air Force Research Laboratory
Air Force Office of Scientific Research
European Office of Aerospace Research and Development
Unit 4515 Box 14, APO AE 09421

REPORT DOCUMENTATION PAGE

PLEASE DO NOT RETURN YOUR FORM TO THE ABOVE ORGANIZATION.

1. REPORT DATE	2. REPORT TYPE	3. DATES COVERED	
20220310	Final	START DATE 20190901	END DATE 20211130

4. TITLE AND SUBTITLE
Simultaneous and Synchronous Full Field Deformation and Temperature Measurements in High Rate Events

5a. CONTRACT NUMBER	5b. GRANT NUMBER	5c. PROGRAM ELEMENT NUMBER
	FA9550-19-1-7016	61102F
5d. PROJECT NUMBER	**5e. TASK NUMBER**	**5f. WORK UNIT NUMBER**

6. AUTHOR(S)
Mikko Hokka

7. PERFORMING ORGANIZATION NAME(S) AND ADDRESS(ES)	8. PERFORMING ORGANIZATION REPORT NUMBER
Tampereen korkeakoulusäätiö sr Kalevantie 4 TAMPERE, Pirkanmaa 33100 FI	

9. SPONSORING/MONITORING AGENCY NAME(S) AND ADDRESS(ES)	10. SPONSOR/MONITOR'S ACRONYM(S)	11. SPONSOR/MONITOR'S REPORT NUMBER(S)
EOARD UNIT 4515 APO AE 09421-4515	AFRL/AFOSR IOE	AFRL-AFOSR-UK-TR-2022-0031

12. DISTRIBUTION/AVAILABILITY STATEMENT
A Distribution Unlimited: PB Public Release

13. SUPPLEMENTARY NOTES

14. ABSTRACT
See report for details.

15. SUBJECT TERMS

16. SECURITY CLASSIFICATION OF:			17. LIMITATION OF ABSTRACT	18. NUMBER OF PAGES
a. REPORT	b. ABSTRACT	c. THIS PAGE		
U	U	U	SAR	10

19a. NAME OF RESPONSIBLE PERSON	19b. PHONE NUMBER *(Include area code)*
DAVID SWANSON	785-6565

Grant no: FA9550-19-1-7016

Title: Simultaneous and Synchronous Full Field Deformation and Temperature Measurements in High Rate Events

PI: Professor Mikko Hokka

Reporting period: September 2019 to February 2022

Summary

From the scientific point of view the work has been very successful. The results have been reported in a chapter in a text book, several scientific journal publications, and in a PhD thesis. The main practical goal of the work was to develop new measurement methods, which now has been completed and validated. The work has raised interest in the scientific community. From the material point of view the basic part of the project and the Option1 covered characterization of several materials, but at this point some of the results are not published yet, and more work and experiments would still be needed to finalize the originally planned research. The main findings of are given here, but a curious reader is referred to the references [1-5] for more details.

- We were successful in carrying out experiments at 1350 °C at the strain rate of approximately 1600 s^{-1} for commercially pure titanium. This experiment was imaged with optical and infrared cameras, and we were able to carry out the full field analysis for the image data. This far exceeds the aims and goals outlined in the research plan.
- We carried out detailed analysis of the error sources and quantified the resolution and accuracy of the measurement as outlined in the research plan.
- We characterized the full thermomechanical behavior of the selected materials as specified in the original research plan.
- We are still carrying out experiments and will focus on inverse modeling approaches to quantify the material response. The research is therefore ongoing, but won't be reported here in details.

Introduction

High strain rate deformation is very important for various military and civilian applications. Various impact events, blast, and explosions are typical military examples where high rate deformation occurs. For civilian applications, numerous forming and machining operations of metals induce large strains at a high rate. In any case, the material behavior, strength, ductility, shear localizations, and energy absorption are strongly influenced by the deformation rate. Because of this, engineers and scientists have tried to collect high quality data from high temperature dynamic tests, but unfortunately, with rather poor success. The main problems associated with the measurements of high rate material deformation include inhomogeneous material flow and adiabatic heating. The goal of this project was to develop a precise measurement that provides accurate information of forces, deformation, and temperature at high spatial resolution with microsecond time resolution. The optical strain measurements using Digital Image Correlation and fast Infrared thermal cameras were used for full field simultaneous deformation and strain measurements. During the course of the project, we have also determined the Taylor-Quinney coefficient of the test material as a function of strain, strain rate, and test temperature at high spatial resolutions.

Methods, Assumptions and Procedures

For the sake of brevity, only a short summary of the experimental setup and the studied materials is given here. More details, more experiments at different strain rates and temperatures etc. are given in refs. [1-5]

A commercially pure α-titanium alloy was used in this investigation, and special dog-bone tensile samples were machined from a 2mm thick sheet using electric discharge machining. The tensile tests were conducted with a tensile Split Hopkinson Pressure Bar (SHPB) device with a direct electric heating system, which enables rapid heating of the sample to the test temperature. The tensile SHPB comprised a steel incident bar, an aluminium bar, and a tubular striker which is accelerated using compressed air. The stress pulses in the incident and transmitted bars were measured by two 5 mm strain gages, amplified by a signal conditioner, and recorded on a digital oscilloscope.

The heating system comprises a welding transformer and pneumatic actuators which grip the sample. The welding transformer passes a current through the gauge section of the specimen and the pneumatic actuators disengage the specimen just moments before the loading pulse reaches the specimen. Due to the short time that the specimen stays at the elevated temperatures, the heat diffusion to the bars is greatly diminished, the oxidation of specimen surface is decreased, and the applied contrast patterns remain ductile on the specimen surface for a longer time and can follow the deformation of the tensile specimen. The tests were conducted at strain rates from 1000 to 1600 s^{-1} and temperatures from room temperature up to 1350 °C.

The tests were monitored by two Photron SA-X2 high-speed cameras and a Telops FAST-IR-M2K high speed infrared camera. All cameras acquired images at a rate of 62 kHz. The optical cameras imaged one side of the specimen with a random pattern prepared on the surface, while the infrared camera imaged the opposite side of the specimen where the surface was only ground and clean. Cold LED lights were used to illuminate the specimen for the optical imaging.

The radiometric temperature values from the infrared camera consider an emissivity of a perfect black body, or a constant determined by the user, and thus had to be converted to true surface temperatures. This calibration was done by monitoring the cooling down of hot specimens simultaneously with a spot welded type K thermocouple and the infrared camera. The strain and temperature on both sides of the specimen were considered to be the same, as the specimens were thin metal sheets. A Keysight 33500B waveform generator and an analog gate were used to synchronize the data acquisition of all measurement systems. The waveform generator sends TTL pulses that clock the optical cameras and triggered the image acquisition of the infrared camera. The analog gate prevents the TTL pulses from reaching the infrared camera until the gate is opened by the oscilloscope trigger out signal. A general view of the experimental setup is shown in Figure 1.

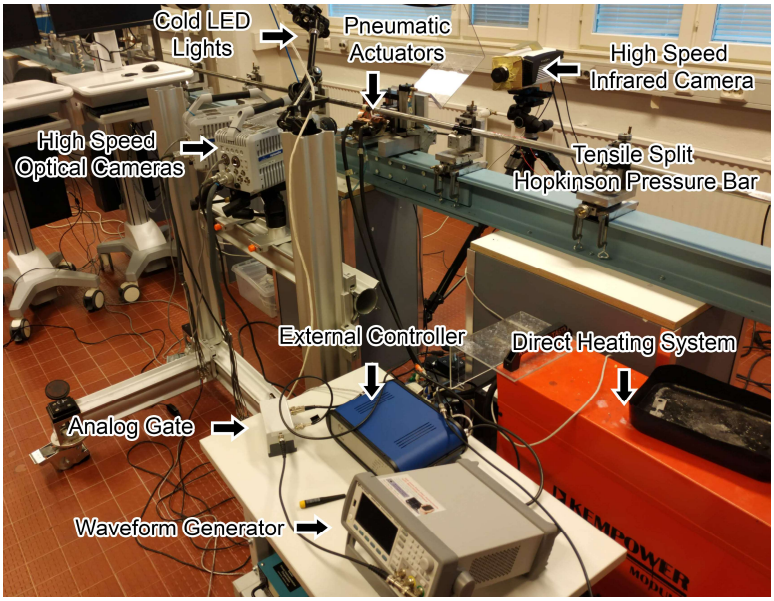

Fig. 1. Experimental setup used for the high temperature tests comprising the direct electric heating system, the high-speed infrared, and optical cameras, and the tensile SHPB.

A random speckle pattern was applied to one side of the sample using a temperature resistant manifold spray paint which resisted temperatures up to 1120 °C. Despite most of the pattern evaporated at the temperature of 1350 °C, DIC measurements were still possible using the remnants of the spray-painted pattern and the surface texture caused by plastic deformation. A bandpass filter (410–570 nm) was used with the optical cameras to filter most of the incandescent radiation emitted by the specimen at elevated temperatures. An attenuation filter had to be used with infrared camera so that imaging of a higher temperature range would be possible. The infrared camera had to be refocused after the attenuation filter was applied and this was done by pursuing sharp edge while imaging a hot soldering iron.

A two-level double-sided 3D calibration plate was used to calibrate all three cameras to a single pinhole model, making it possible to overlap the images from both optical and infrared cameras by representing both datasets in the same world coordinate system. Considering that the attenuation filter changes the optics of the infrared camera, the infrared images of the calibration plate had to be taken while having the filter equipped. The calibration plate could not be heated up so that it would emit enough radiation to be imaged by the infrared camera, and therefore an approach of using reflected infrared radiation from the surface of the calibration plate was used. Non-Uniformity Correction (NUC) maps were used to acquire these images, as they allowed for better intensity imaging of the calibration plate through the attenuation filter. Adequate results were obtained by using either a ring-shaped heater or an infrared bulb, but the former was chosen as it produced less shadows.

The IRT images were deformed using the displacement vector fields obtained from DIC so that both temperature and strain data could be analysed in the reference frame of the undeformed sample. At elevated temperatures, the specimens did not always break during the first loading pulse. However, it was possible to obtain full-field information from the sample during the second loading pulse as well and measure the full-field strain/temperatures up to the rupture of the specimen. These results were represented as full-field maps overlayed on top of the optical images and as 3D waterfall plots which allowed for an easier comparison of the results at different testing conditions. The noise-floor of the strain and displacement measurements of DIC doubled at higher temperatures but stayed within an acceptable range.

Results and Discussion

The mechanical strength of the material decreased drastically at elevated temperatures while the ductility increased, mostly due to a much higher non-uniform deformation. At higher temperatures, necking was very pronounced and started at the very beginning of plastic deformation. The strain localization at elevated temperatures is much higher than that at room temperature. The evolution of the full field strains and temperatures as a function of engineering strain for a sample tested at an average temperature of 1350°C and a strain rate of 1600 s^{-1} is shown in Figure 2. Even though most of the contrast pattern evaporated at this temperature, the reimaging pattern and the surface features allowed for strain measurements to be made. Axial strain mostly concentrated on the hotter parts of the specimen and no discernible adiabatic heating was observed under these conditions.

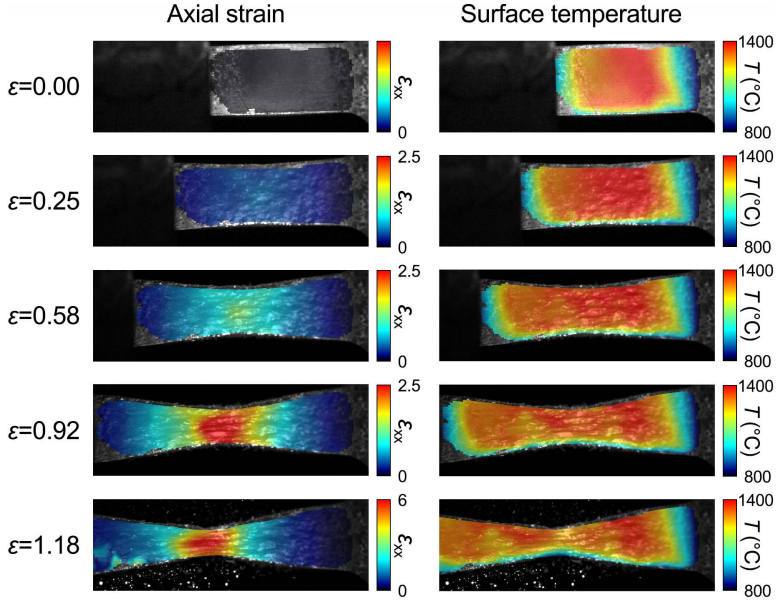

Fig. 2: Full-field axial strain and temperature maps overlayed on the optical images of the specimen at different overall engineering strains of a commercially pure titanium specimen tested in tension at a strain rate of 1600 s^{-1} and an initial temperature of approximately 1350 °C.

The full-field data from the same test at 1350 °C is further presented in Figure 3 as 3D waterfall plots where strain and temperature are shown as a function of position along the gage length of the specimen and global engineering strain. The highest measured local axial strain was of almost 10. The specimen had a temperature gradient throughout its gauge length prior to testing, and while the average temperature did not change during the test the temperature data obtained in some regions was less stable during the experiment at these extreme conditions. This could possibly be caused local changes in the emissivity of the surface caused by the plastic deformation and oxidation. There was no noticeable relationship between the strain and temperature evolution in the test at 1350 °C. The darker line in the plot at an engineering strain of approximately 1, originates from the data obtained from the pictures that were taken in between loading pulses during which the specimen was not loaded. It is also evident from this plot that there is no considerable decrease in temperature between the loading pulses. Presenting the full-field data as 3D waterfall plots allow for data from all acquired images to be observed at a quick glance and makes it easier to compare the strain localization and adiabatic heating among different testing conditions and materials.

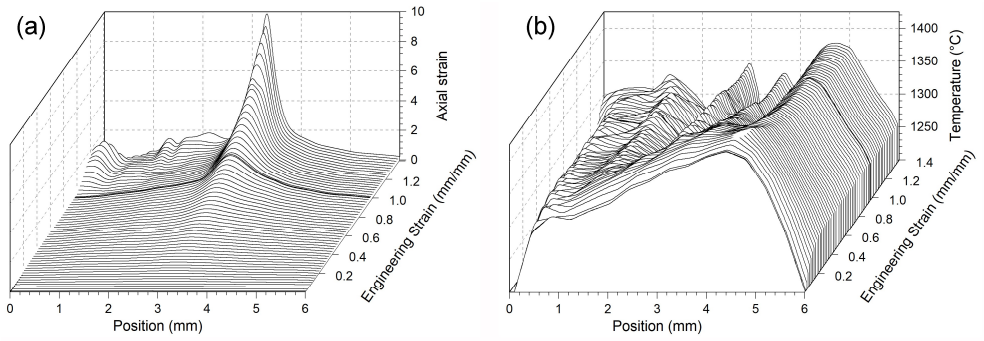

Fig. 3: 3D waterfall plots of axial strain and temperature as a function of position along the gage length of the specimen and global engineering strain of a commercially pure titanium specimen tested in tension at a strain rate of 1600 s^{-1} and an initial temperature of approximately 1350 °C.

Another compelling form of presenting such full-field data in an even more compact manner is a surface plot where axial strain is shown as a function of position along the gage length and global engineering strain, and where the local temperature is represented by the colour. Figure 4 shows an example of such a plot which illustrates the strain and temperature evolution of a specimen tested at an initial temperature of 700 °C and a strain rate of 1600 s^{-1}. This plot shows well that both the full-field strain and temperature data are temporally and spatially synchronized, and properly presented on the same frame of reference. Although this test was carried out at elevated starting temperature, considerable adiabatic heating was observed first throughout the gage length of the specimen and later concentrated on the necking region only. Increasing temperature was observed up to an axial strain of 2, but the adiabatic heating slowed down significantly even when the localization became more evident. Strain localization at 700 °C is smaller than at 1350 °C and the maximum local axial strain were of approximately 4.5.

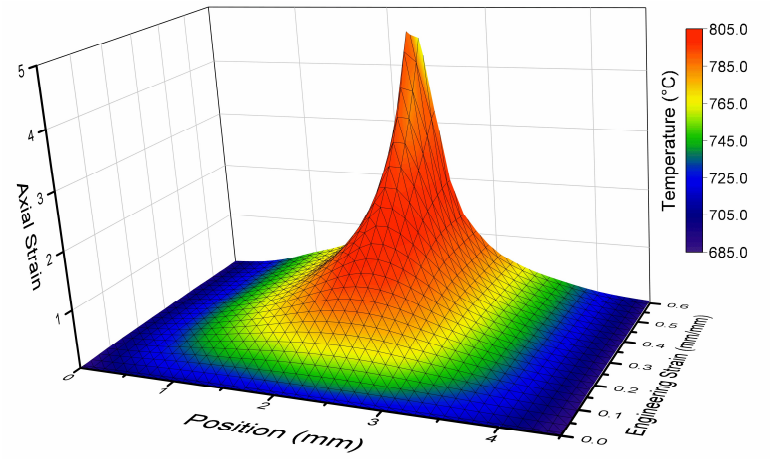

Fig. 4 Surface plot of local axial strain as a function or position along the gauge length and global engineering strain of a specimen under tension at a strain rate of approximately1600 s^{-1} and an initial temperature of 700 °C. The plot is colour coded so that it possible to visualize the local surface temperature of the specimen in the same representation as the local axial strain.

The uncertainties of displacements and strains measured by DIC were evaluated by averaging 10 stationary images of the unloaded sample at different temperatures and analyzing the standard deviation of these displacement, strain, stereo reconstruction error, and radiometric temperature. In such conditions, there should not be any detectable strains and any measured strain would be associated with external uncertainty sources. The stereo reconstruction error (epipolar error) at different testing temperatures was also evaluated from the stationary images and are shown as an average and standard deviation as a function of radiometric temperature. Considering that the sample is virtually at the same temperature if imaged at a very high acquisition rate, the noise floor of the full-field temperature measurements was evaluated by averaging 10 thermal images of the heated sample shortly before the dynamic loading. These images were taken in approximately 160 μs, and the heat diffusion during that time is very low. The radiometric temperature resolution was considered as the standard deviation of the radiometric temperature in the gage length of the specimens. Figure 5 shows the resolution of the displacement, strain, and temperature full-field measurements, as well as the average stereo reconstruction error as a function of the radiometric temperature. In all cases the measured mean strain values were practically null. Furthermore, displacement, strain and temperature noise-floors were considerably lower than the quantities-of-interest observed during deformation. Although stereo reconstruction error showed a much higher standard deviation at higher temperatures in comparison with that at room temperature, it was only twice as high at the highest investigated temperature. The decrease in the strain and displacement resolution, and the increase of the stereo reconstruction error with increasing temperature could be associated with many factors, such as distortions caused by heated air in the vicinity of the hot specimen, degradation of the pattern due to the high temperature, and interference of the incandescent radiation in the gray levels recorded by the optical cameras. However, considering

that only a small section of the specimen is at the testing temperature, the uncertainties caused by the air distortions should be lower than for testing systems where more elements of the setup are at high temperatures. The increase in the resolution of the radiometric temperature is probably related to the better signal-to-noise ratio at higher temperatures. In addition, according to the infrared camera manufacturer, the maximum expected uncertainty for the temperature measurements is of ±1°C or ±1% from 0 to 200°C and 2°C or ±2% from 200 to 1500°C. Therefore, the highest expected deviation at the highest radiometric temperature investigated in this work, would be of approximately 20 °C. The overall resolution and accuracy of the method seem quite reasonable for most high strain rate materials science and engineering research.

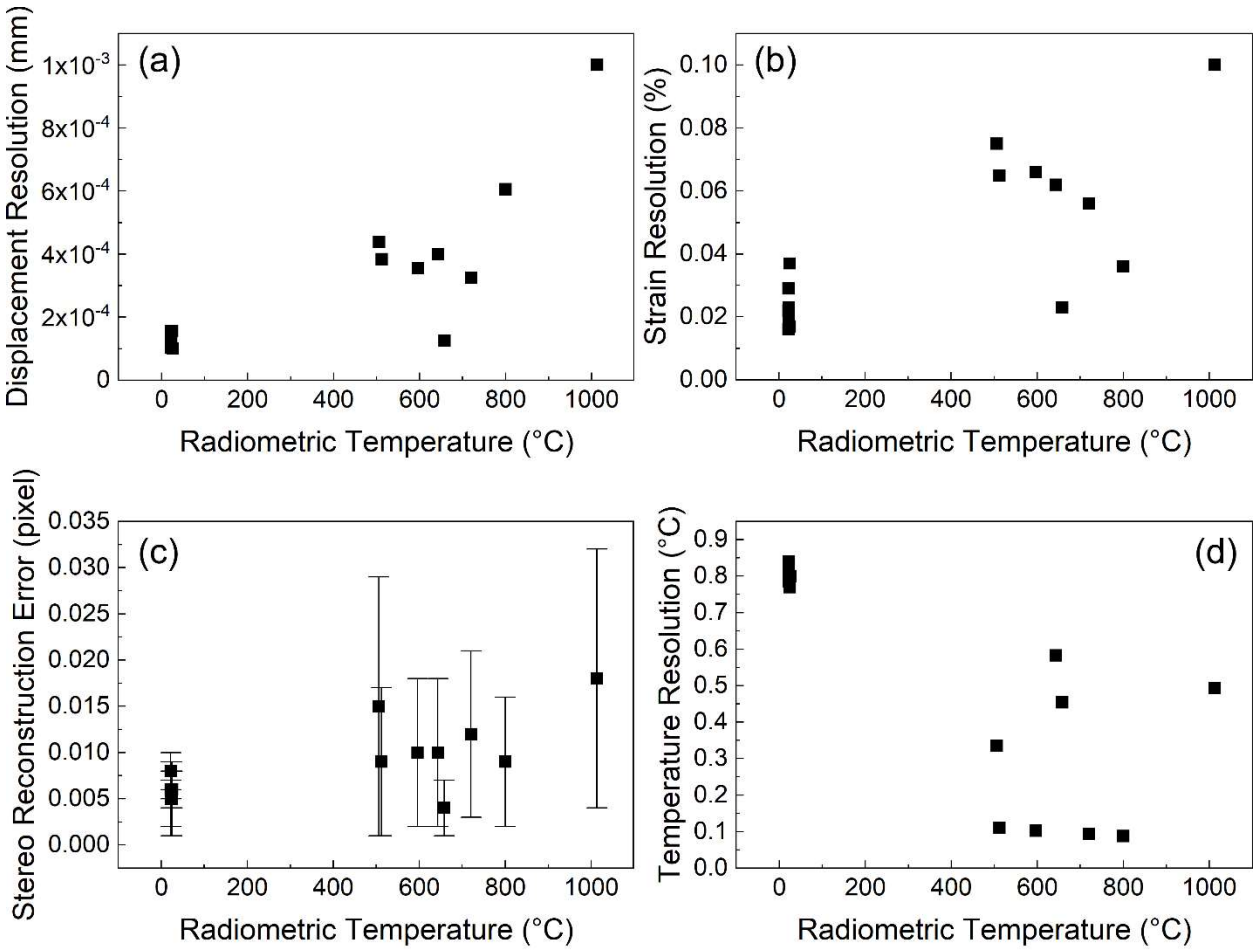

Fig. 5 Uncertainties of the full-field quantities-of-interest of the DIC and IRT measurements as a function of radiometric temperature. (a) Displacement, (b) strain, (c) stereo reconstruction error, and (d) radiometric temperature. The error bars represent the standard deviation of the stereo reconstruction error throughout the sample gage length

Conclusions

In this project we have developed a method for full-field strain and temperature measurements for materials tested at high temperature and high strain rate by integrating synchronized DIC and IRT, an electrical resistive heating system, and a tensile SHPB. In this report we have shown as an example the full-field thermomechanical characterization of commercially pure titanium at strain rates up to approximately 1600 s^{-1} and temperatures up to 1350 °C. More details are given in the referred articles. We would like to highlight the following novelties:

- The full-field strain and temperature measurements of high strain rate tension tests for titanium at elevated temperatures were successfully temporally and spatially synchronized. The strain and temperature evolutions during uniform deformation and necking of titanium at elevated temperatures were monitored with high temporal and spatial resolution.
- A decrease in mechanical strength and increase in ductility were observed with increasing temperature. The local strains in the neck also increased considerably with temperature. The critical strain at which the rate of strain localization increased rapidly was higher at higher testing temperature.
- A temperature increase as high as 80 °C was observed at 700 °C despite the low strength of the material and consequent low applied mechanical work. A decrease in the radiometric temperature was observed during necking at 700 °C, which can at least partly be explained by a local decrease in emissivity due to the massive strain localization after reaching approximately 200% axial strain. No considerable adiabatic heating was observed at higher testing temperatures.
- The resistive electric heating generated a temperature gradient along the gage section of the specimen, but as the strength of the material at 1120 °C does not strongly depend on temperature, the specimen deformed throughout the gage length of the specimen. At 700 °C the material response depended on the temperature more strongly, and the necking was more localized even though the gradient was smaller.
- A blue-green shortpass filter and high temperature resistant engine manifold spray paints were used to enable DIC at high temperatures where the material is incandescent. High temperature infrared intensity filter was used enable IRT data acquisition at a wide range of temperatures. The contrast of a painted pattern imaged with the shortpass filter was reduced by 50% at a temperature of 880 °C, but still retained sufficient contrast for DIC.
- Calibration curves were constructed to convert radiometric temperature values to true surface temperature values by monitoring the temperature of a cooling sample with the infrared camera and thermocouples. An extra temperature calibration curve and an integrated calibration approach were used to address the substantial drop in radiometric temperature caused by the formation of a rougher surface texture during deformation in a given range of temperatures.
- The uncertainties of DIC and IRT were evaluated as a function of testing temperature, and while there was a decrease in the displacement and strain resolution with temperature, they are still adequate for the measurements at elevated temperatures.

This method looks very promising for studying material behavior in applications where high strain rates occur at high temperatures, as the acquired data can be used for constitutive modelling, finite element analysis, and inverse modeling approaches. Furthermore, this method produces additional data that facilitates the description of the material behavior, especially for such materials where the onset of necking occurs very quickly after yielding. The full-field approach complements the standard Hopkinson Bar analytics with local strain and temperature information. The full-field techniques are going to play an important role in furthering our understanding on necking, strain localization, failure mechanisms and its relationship with material properties under extreme conditions.

References

[1] G. Soares, N.I. Vazquez, M. Hokka, Thermomechanical behavior of steels in Tension studied with synchronized full-field deformation and temperature measurements. Experimental Techniques (2021), vol. 45; pp 627-643.

[2] G.C. Soares, N.I. Vázquez-Fernández, M. Hokka, "Simultaneous full-field strain and temperature measurements in high strain rate testing", in "Advances in Experimental Impact Mechanics", *Elsevier*, Amsterdam, pp. 255–285, (2022).

[3] G. C. Soares and M. Hokka, "Simultaneous Full-field Strain and Temperature Measurements in High Strain Rate Tensile Hopkinson Bar Experiments at Elevated Temperatures", EPJ Web of Conferences, vol. 250, pp. 01015, (2021).

[4] G. C. Soares and M. Hokka, "Synchronized Full-Field Strain and Temperature Measurements of Commercially Pure Titanium under Tension at Elevated Temperatures and High Strain Rates", Metals, accepted for publication and available online, 2022. https://www.mdpi.com/2075-4701/12/1/25/pdf

[5] G. C. Soares, Thermomechanical Behaviour of Materials under Extreme Conditions Studied with High Speed Optical and Infrared Imaging, a thesis presented for the degree of Doctor of Technology; thesis submitted for evaluation 2021.